

# MULTISTATIC RADAR CHANGE DETECTION USING SPARSE IMAGING METHODS

Mike Brennan, Chris Kreucher, and Ben Shapo

Integrity Applications Incorporated  
Ann Arbor MI

## ABSTRACT

This paper describes a sparse imaging approach for estimating change images from a multistatic radar data. In our application, antennas are arranged around the perimeter of a surveillance region. This provides large angular diversity but a very small angular sampling over the large aperture. Furthermore, due to application constraints, the scene is interrogated with limited frequency diversity. We address the change image estimation problem using a compressed sensing reconstruction method to estimate the high-dimensional signal from the much lower dimensional measurement. We show with real collected data the sparseness model enables excellent imaging with very limited spatial and frequency sampling.

**Index Terms**— multistatic radar, change imaging, narrowband, compressed sensing, sparse model estimation

## 1. INTRODUCTION

Compressed sensing, the problem of estimating a sparse signal  $\underline{x} \in \mathbb{C}^n$  from a much smaller number of samples  $\underline{b} = \underline{A}\underline{x} \in \mathbb{C}^k$ ,  $k \ll n$ , has recently received increased attention from the statistical signal processing community [1]-[2]. It is motivated by the fact that in many applications high-dimensional signals are well described with a small number of coefficients in an appropriate basis. This allows reconstruction of a signal from much fewer measurements than ordinary Nyquist criteria would require.

This paper describes an application of compressed sensing methods to data collected by a multistatic radar array. In our application, we estimate a high-resolution spatial change image from a small set of frequency response measurements. We are interested in imaging with a small spectral footprint, since oftentimes the frequency spectrum is occupied by other sources, leaving only a small portion available for our use. We employ a constellation of geometrically diverse radar as one means of mitigating the lack of spectral diversity.

We form change images between reference and test collections. This setting ensures the image will be sparse in the  $XY$  pixel domain and motivates a sparseness model on the estimate. Data is collected with a step-frequency radar, which uses a gated CW pulse with low instantaneous bandwidth.

This work was supported by AFRL contract FA8650-10-C-1718.

Traditionally, such a radar is swept through a large range of frequencies at small intervals to simulate a wide bandwidth chirp. Our application uses a small number of random frequency samples (each with a small instantaneous bandwidth) and illustrate that the sparsity model allows for excellent recovery of the unknown change image.

## 2. SPARSE MODEL IMAGING FORMULATION

We construct a change image over an  $XY$  region from data collected before and after a change. This section develops the notation and mathematics describing the approach. Section 3 illustrates the algorithm on real, collected field data.

### 2.1. The Received Data

Our experiments use an AKELA AVMU500A radar, which is a stepped-frequency continuous wave (SFCW) radar. A SFCW measures the scene frequency response at a discrete set of frequencies by sequentially stepping the transmitter through frequency. The signal source dwells at each frequency long enough to allow echoes from the scene to reach the receiver and then mixes the return with the transmitted signal. The resulting measurements can be viewed as a complex signal representing the frequency response of the scene at  $N_f$  discrete frequencies  $f_1, \dots, f_{N_f}$ .

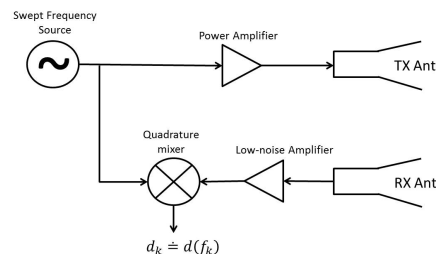


**Fig. 1:** Nominal Stepped-frequency Continuous Wave Radar

The AKELA radar is programmable and capable of transmitting between 300MHz and 3GHz. The rate at which the individual frequencies are sampled is selectable, and set here at 45kHz. This pulse length defines the instantaneous bandwidth of the transmitter. The radar has four ports, any of which may be used for transmit or receive; however, because

the radar has only one transmitter and receiver, it is not possible to receive multiple ports simultaneously. Therefore the collections transmit and receive between one pair, and then move to transmit and receive to the next pair, and so on.

## 2.2. Estimate and Measurement Notation

The surveillance region is discretized into a set of pixels. For the purpose of exposition, we assume the region is rectangular and evenly sampled, defined by  $x \in x_{min}, x_{max}$ ,  $y \in y_{min}, y_{max}$ , and grid spacing  $\delta x$  and  $\delta y$ . Let  $N_x$  and  $N_y$  be the number of grid points in the  $X$  and  $Y$  directions, respectively. The surveillance region then has  $N_x N_y$  pixels, each of which contains an unknown change we wish to estimate from data collected before and after the change.

Let  $\underline{x}$  denote the  $N_x N_y \times 1$  vector of unknowns, which will be organized  $x$ -coordinate major, i.e.,

$$\underline{x} \leftrightarrow \begin{bmatrix} x_{min}, y_{min} \\ x_{min}, y_{min} + \delta y \\ \vdots \\ x_{min}, y_{max} \\ x_{min} + \delta x, y_{min} \\ \vdots \\ x_{min} + \delta x, y_{max} \\ \vdots \\ x_{max}, y_{max} \end{bmatrix}, \quad (1)$$

so the  $j^{th}$  element ( $j = 1, \dots, N_x N_y$ ) of  $\underline{x}$ , denoted  $x_j$ , corresponds to a cell centered at

$$\begin{aligned} x_j &= x_{min} + \delta x \lfloor (j-1)/N_y \rfloor \\ y_j &= y_{min} + \delta y \text{rem}(j-1, N_y). \end{aligned} \quad (2)$$

Multistatic radar measurements are made by the constellation both before and after a change. Let  $N_P$  be the number of transmit/receive pairs. The raw frequency response measurement vector is a set of  $N_f$  complex numbers for each of the transmitter/receiver pair (assumed to be the same for each pair for notational convenience). The measurements used by the algorithm are the complex-valued, range-filtered, frequency response differences from before and after the change.

Formally, the range-filtered received data at frequency bin  $f_k$  from pair transmit/receive  $p$  will be denoted  $d_k^p$ , and the change in measurements from before and after a change at frequency bin  $f_k$  from pair  $p$  will be denoted  $\Delta d_k^p$ . In practice, this value is computed by averaging over many pulses.

The  $N_p N_f \times 1$  measurement vector  $\underline{b}$  is then the collection of changes  $\Delta d_k^p$ , which will be arranged transmit/receive pair major and frequency-bin minor, i.e.,

$$\underline{b} = \left[ \Delta d_1^1 \cdots \Delta d_k^1 \cdots \Delta d_{N_f}^1 \cdots \Delta d_1^P \cdots \Delta d_{N_f}^P \right]^T \quad (3)$$

The  $i^{th}$  element of measurement vector  $\underline{b}$  corresponds to frequency bin  $\kappa_i$  and bistatic transmitter/receiver pair  $\rho_i$  as

$$\kappa_i = 1 + \text{rem}(i-1, N_f) \quad (4)$$

$$\rho_i = 1 + \lfloor (i-1)/N_f \rfloor. \quad (5)$$

We note also that pair  $\rho_i$  corresponds to a particular transmitter/receiver denoted  $T_i$  and  $R_i$ .

## 2.3. The Measurement Model

We now develop the model of how changes in the surveillance region  $\underline{x}$  are reflected in measurements  $\underline{b}$ . The starting point is a model of how surveillance region changes map to changes in bistatic range, which is the Fourier transform of the measured frequency bin vector. For this purpose, let the vector  $\underline{b}^{range}$  be the  $N_p N_f \times 1$  change in bistatic range measurements which correspond to the  $N_p N_f \times 1$  frequency domain measurement vector  $\underline{b}$ . They are related through the  $N_p N_f \times N_p N_f$  Fourier matrix  $\underline{F}$ , i.e.,  $\underline{b} = \underline{F} \underline{b}^{range}$ .

The  $i^{th}$  element in  $\underline{b}^{range}$  corresponds to range bin

$$\beta_i = 1 + \text{rem}(i-1, N_r). \quad (6)$$

The bistatic radar range equation defines the relationship between the unknowns  $\underline{x}$  and the changes in bistatic ranges  $\underline{b}^{range}$ . For a notional target at  $(x_j, y_j)$ , the received power  $P_r$  is related to the transmitted power  $P_t$  though the wavelength  $\lambda$ , receiver and transmitter gains  $G_t$  and  $G_r$ , target RCS  $\sigma$ , and ranges to the transmitter and receiver  $r^T$  and  $r^R$ :

$$P_r = \frac{P_t G_t G_r \lambda^2 \sigma}{(4\pi)^3 (r^T)^2 (r^R)^2}, \quad (7)$$

and the phase of the received signal depends on the total bistatic range and wavelength as  $(r^T + r^R)/\lambda$ .

In our notation, surveillance region index  $j$  corresponds to the physical location  $(x_j, y_j)$  and measurement index  $i$  corresponds to transmitter  $T_i$  and receiver  $R_i$ . Denote the transmitter and receiver locations by  $(x_{T_i}, y_{T_i})$  and  $(x_{R_i}, y_{R_i})$ . Then the ranges between surveillance region index  $j$  and the transmitter and receiver associated with  $i$  are

$$r_{ij}^T = \sqrt{(x_j - x_{T_i})^2 + (y_j - y_{T_i})^2} \quad (8)$$

$$r_{ij}^R = \sqrt{(x_j - x_{R_i})^2 + (y_j - y_{R_i})^2} \quad (9)$$

The total bistatic range between  $(x_j, y_j)$  and a transmitter/receiver pair specified by  $i$  is  $r_{ij} = r_{ij}^T + r_{ij}^R$ .

The bistatic range  $r_{ij}$  corresponds to bin  $\Gamma_{ij} = 1 + \lfloor \text{rem}(r_{ij}, r_{amb})/\delta_r \rfloor$ , where  $\delta_r$  is the range bin spacing given by the speed of transmission and radar bandwidth ( $\delta_r = c/BW$ ) and  $r_{amb}$  is the maximum unambiguous range, given by the bandwidth and the frequency step ( $r_{amb} = BW/\Delta f$ ).

With this as background, we can now precisely define the response matrix  $\underline{\underline{A}}$ , which is a  $N_P N_r \times N_x N_y$  matrix that maps changes at  $(x_j, y_j)$  locations to observed changes in bistatic range measurements  $\Delta r_k^p$ . The model is

$$\underline{b}^{range} = \underline{\underline{A}} \underline{x} \quad (10)$$

For a test cell  $j$  and transmitter/receiver pair defined by  $i$ , the elements  $\underline{\underline{A}}_{ij}$  reflect the gain and phase due to the bistatic range from the test cell to the pair. It has non-zero elements only when a spatial location implied by  $j$  maps to the bistatic range bin defined by  $i$  in the transmitter/receiver pair defined by  $i$ , i.e., where  $\Gamma_{ij} = \beta_i$ . Let  $r_i^0$  denote the range to scene center for a transmit receive pair indicated by  $i$ . Then, from this analysis, the elements of  $\underline{\underline{A}}$  are

$$\underline{\underline{A}}_{ij} = \begin{cases} G_{ij} \frac{e^{-\sqrt{-1}4\pi f(r_{ij} - r_i^0)/c}}{r_{ij}^T r_{ij}^R} & \text{if } \Gamma_{ij} = \beta_i \\ 0 & \text{otherwise} \end{cases} \quad (11)$$

Where  $G_{ij}$  captures antenna gains, transmit power and other constants. The values are set via a calibration collect. In practice,  $(x_j, y_j)$  does not correspond precisely to a range bin center, and so its energy will spread among neighboring bins. This is approximated in our model by using

$$\underline{\underline{A}}_{ij} = \begin{cases} \alpha_{ij} G_{ij} \frac{e^{-\sqrt{-1}4\pi f(r_{ij} - r_i^0)/c}}{r_{ij}^T r_{ij}^R} & |\Gamma_{ij} - \beta_i| < M \\ 0 & \text{otherwise} \end{cases} \quad (12)$$

where  $M$  is a gate size and  $\alpha_{ij}$  is a weighting representing the fraction of the energy that a scatterer at  $(x_j, y_j)$  puts into the bistatic range bin  $\Gamma_{ij}$ .

This gives the final linear model which completely specifies the relationship between the estimatee  $\underline{x}$  and the frequency-domain measurements  $\underline{b}$  as

$$\underline{b} = \underline{\underline{F}} \underline{\underline{A}} \underline{x} \quad (13)$$

## 2.4. Sparse Imaging Estimation Algorithm

In our application, eq. (13) is an underdetermined linear system, meaning many estimates  $\underline{x}$  will explain the measurements. As a means of selecting the appropriate estimate, we note that the change image  $\underline{x}$  is by its definition sparse. We use this fact to impose a sparseness constraint on  $\underline{x}$  in a basis pursuit (BP) denoising framework to estimate a unique  $\underline{x}$ , i.e., we solve

$$\underset{\underline{x}}{\operatorname{argmin}} \|\underline{x}\|_1 \quad \text{s.t.} \quad \|\underline{\underline{F}} \underline{\underline{A}} \underline{x} - \underline{b}\|_2 < \sigma \quad (14)$$

We use the toolset described in [3] and implemented in a code base called SPGL1. This toolset achieves the solution by solving a sequence of LASSO problems

$$\underset{\underline{x}}{\operatorname{min}} \|\underline{\underline{F}} \underline{\underline{A}} \underline{x} - \underline{b}\|_2 \quad \text{s.t.} \quad \|\underline{x}\|_1 < \tau \quad (15)$$

via a spectral projected-gradient algorithm. Each of the solutions generates an update to a Newton root-finding algorithm that converges on the location where the residual  $\|\underline{\underline{F}} \underline{\underline{A}} \underline{x} - \underline{b}\|_2$  is below the noise tolerance parameter  $\sigma$ . The parameter  $\sigma$  defines the tolerable difference between the change image prediction of differences in bistatic range measurements and the actual measured differences. For this reason, it is typically referred to as the noise parameter.

## 3. EXPERIMENTAL RESULTS

We illustrate our approach with a field collect. Figure 2 shows a four-element RF array where data was collected from each of the 6 unique bistatic pairs using the AKELA SFCW Radar described earlier. The collection used 1500 evenly spaced frequency steps between 1 and 3 GHz. The radar hopped frequencies every  $22\mu s$ , giving each pulse approximately  $45kHz$  instantaneous bandwidth. Therefore, although the total bandwidth was  $2GHz$ , significant energy was only transmitted into  $70MHz$  ( $= 1500 \times 45000$ ) of the spectrum.

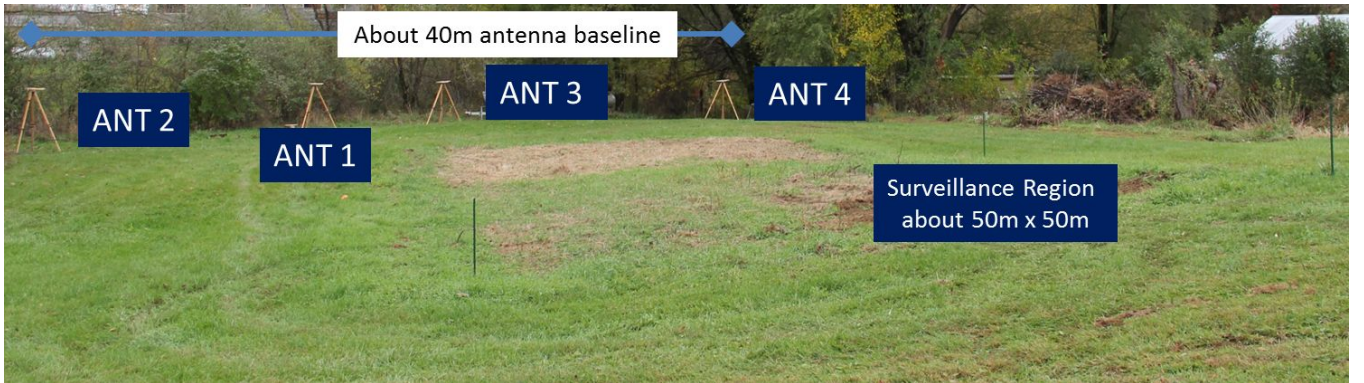


**Fig. 2:** Imaging Area, Showing 4 Antennas Forming a 40m Baseline and a 50m × 50m Surveillance Region

Data was recorded before and after the change shown in Figure 3, where two cylinders were added at about 30m stand-off from the array.



**Fig. 3:** Top: The Region Before and After the Change.

Figure 4 shows the change images estimated on a  $901 \times 601$  grid. There were  $6 \times 1500$  frequency measurements collected, meaning there are about 60 times as many estimates as measurements. The top panel shows the original collect produces a sharp estimate of the two changes. The middle and bottom panels show excellent imaging still results with dramatically fewer frequency samples. The middle panel shows the change image with 40% of the samples discarded (in practice, these would never have been collected). The bottom panel shows the change image with 90% of the samples discarded. The image still clearly shows the change locations.

#### 4. CONCLUSION

This paper has described and illustrated a sparse imaging approach for change image estimation using a multistatic radar array. We've given an algorithm that uses a compressed sensing reconstruction approach and radar signal models to estimate reflectivity changes in a region. We've shown experimentally that the scene sparsity enables recovery of useful change images with a very small number of frequency samples. Future work includes determining the minimum number of samples and their character required for good imaging.

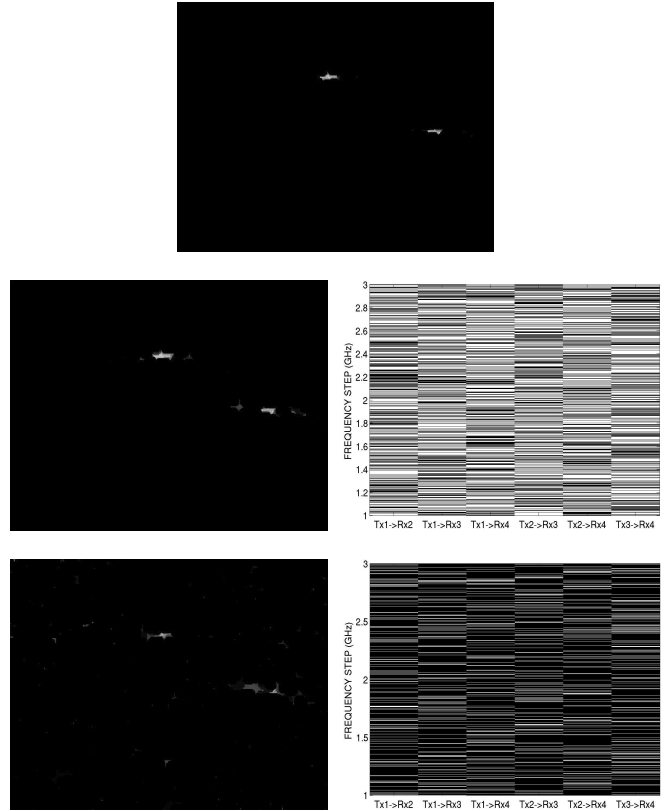


**Fig. 4:** Top: Change Image Using 1500 Step Frequencies from each of the 6 Unique Bistatic Pairs. Mid: Image When Randomly Discarding 40% of the Measurements, and Which Measurements Were Discarded. Bot: Image When Randomly Discarding 90% of the Measurements, and Which Measurements Were Discarded.

#### 5. REFERENCES

- [1] Y. Yeo-Sun and M. Amin, "Imaging of behind the wall targets using wideband beamforming with compressive sensing", *IEEE Statistical Signal Proc. Workshop*, 2009.
- [2] E. Vera, L. Mancera, S. Babacan, R. Molina, and A. Katsaggelos, "Bayesian Compressive Sensing of Wavelet Coefficients Using Multiscale Laplacian Priors", *IEEE Statistical Signal Processing Workshop*, 2009.
- [3] E. van den Berg and M. Friedlander, "Probing the Pareto frontier for basis pursuit solutions", *SIAM J. on Scientific Computing*, 31(2):890-912, November 2008.
- [4] D. Malioutov and M. Cetin and A. S. Willsky, "A sparse signal reconstruction perspective for source localization with sensor arrays", *IEEE Trans. Signal Processing*, vol. 53, no. 8, Aug. 2005, pp. 3010-3022.